Clinicopathological, immunohistochemical and molecular features of acinic cell carcinoma of the breast

XINHUA YANG[1], FANGYUN LIU[2*], CONGYANG LI[3*], ZUO LI[4*], PEIPEI WANG[5], MENG ZHANG[3], YANFENG LIU[3], CAIWEN ZHOU[3], YUYING LI[6], ZHENZHEN CHAI[6], XIAOGUANG GU[7], XUEQING XIAO[8] and GUOXIA LI[9]

[1]Department of Oncology, People's Liberation Army 989 Hospital, Pingdingshan, Henan 467000; [2]Department of Pathology, Hangzhou Fenlan Medical Laboratory, Hangzhou, Zhejiang 310056; Departments of [3]Pathology, [4]Endocrinology, [5]Radiology, [6]Ultrasonics, [7]General Surgery and [8]Medical Area, People's Liberation Army 989 Hospital, Pingdingshan, Henan 467000; [9]Department of Pathology, Minhang Hospital, Fudan University, Shanghai 201199, P.R. China

Received May 5, 2023; Accepted October 31, 2023

DOI: 10.3892/ol.2024.14241

Abstract. Breast acinic cell carcinoma (ACC) is a rare subtype of breast cancer. Accurate diagnosis of ACC using core needle biopsy (CNB) is pivotal for the use of effective treatments and patient prognosis. In the present study, a detailed analysis of the morphological, immunohistochemical and gene mutation features of 2 cases of ACC was performed. CNB was performed prior to surgical excision. The breast ACC in the present cases exhibited overt burrowing labyrinthine networks or 'hand-holding-hand' features. The tumor cells in both of the present cases expressed cytokeratin (CK)7, S100 and CK5/6, but were negative for p63, estrogen receptor and progesterone receptor. GATA binding protein 3 was positive in case 1 but negative in case 2. Fluorescence *in situ* hybridization indicated no ETS variant transcription factor 6 break-apart probe detection. Next-generation sequencing results revealed the same mutation and a similar abundance in exon 27 (NM_005120.2; c.3817G>T; p.A1273S) of the mediator of RNA polymerase II transcription, subunit 12 homolog (*MED12*) gene in both patients. To conclude, the findings of the present study suggested that recognition of this rare 'hand-holding-hand' structure could potentially be beneficial for avoiding patient misdiagnosis. In addition, it could be suggested that a mutation in the *MED12* exon 27 was associated with the formation of a burrowing labyrinthine network or 'hand-holding-hand' feature.

Correspondence to: Dr Xueqing Xiao, Department of Medical Area, People's Liberation Army 989 Hospital, 44 Jianshe Road, Pingdingshan, Henan 467000, P.R. China
E-mail: 361035348@qq.com

Professor Guoxia Li, Department of Pathology, Minhang Hospital, Fudan University, 170 Xinsong Road, Shanghai 201199, P.R. China
E-mail: gxliben97@163.com

*Contributed equally

Key words: acinic cell carcinoma, breast cancer, mediator of RNA polymerase II transcription, subunit 12 homolog

Introduction

Breast cancer is the most commonly diagnosed cancer worldwide in women in 2020, with an estimated 2.3 million new cases (11.7% of cancer cases in female patients), followed by lung cancer (11.4%) (1). Acinic cell carcinoma (ACC) is characterized by the presence of cancer cells with diffuse serous differentiation (2,3). ACC can occur in the salivary glands, pancreas, lung, stomach and breast (2-8). Breast ACC is a rare subtype of breast cancer that has a benign course in the majority of cases (8), although occasionally it can progress into high-grade triple-negative breast cancer (TNBC) (9,10). Although typically characterized by the presence of cells with diffuse serous differentiation, breast ACCs can differ both histologically and molecularly (8,9). Breast ACCs are frequently found to comprise cytologically bland cells with abundant eosinophilic cytoplasm, containing coarse or fine zymogen-like cytoplasmic granules (8,9). These granules tend to arrange themselves into a mixture of infiltrative microglandular and nested growth patterns (10).

A previous genomic analysis study reported that breast ACCs are not related to their salivary gland counterparts, instead being closer to microglandular adenosis in addition to sharing a similar molecular profile to TNBC (11). Tumor protein p53 (*TP53)* mutations appear to be the most consistent molecular event in ACC (11). *PI3Kα* mutations, BRCA1 DNA repair-associated gene alterations, such as mutations and gene deletions, and MutL homolog 1 germline mutations have also been described in a subset of ACC cases (11,12).

Compared with open biopsy, image-guided core needle biopsy (CNB) is highly sensitive and specific for the diagnosis of breast cancer, leading to its widespread application (13). However, due to the low incidence rate of ACC and lack of clinicopathological information present in the biopsy tissues, breast ACC can be difficult to differentiate from invasive breast carcinoma of no special type (NST) and other types of TNBC pre-operatively (14). ACCs frequently exhibit a TNBC

phenotype but less aggressive clinical behavior compared with the NST subtype (15). Therefore, the present study aimed to analyze the morphological and immunohistochemical features of breast ACC tumor samples obtained by CNB and surgical excision. The association between the genomic landscape and the morphological features of breast ACCs was also investigated using next-generation sequencing (NGS).

Patients and methods

Patients. The clinical data from the medical records of 2 patients (case 1 and case 2) diagnosed with breast ACC were retrospectively reviewed. Image-guided CNB was performed before surgical treatment between January 1, 2015 and December 31, 2022. The cases originated from the Department of Pathology of the People's Liberation Army 989 Hospital (Pingdingshan, China) or the Fenlan Laboratory (Hangzhou, China). The cases were reviewed by five of the authors and samples were anonymized prior to analysis. The present study was approved by 989 Hospital Medical Ethics Committee (approval no. WZLL-2023-016) and Fenlan Lab Medical Ethics Committee (2023-06). Patient consent was obtained if required by the protocols. All tissues were fixed in 10% formalin at room temperature for 24 h. For each tissue specimen, 4-μm sections were cut. Hematoxylin and eosin-stained sections at room temperature for 15 min of each case were reviewed by three pathologists (LCY, LFY and LGX) under the BX53 light microscope (Olympus Corporation). The inclusion criterion was a diagnosis in accordance with breast ACC.

Immunohistochemistry (IHC). Biopsy and surgical tissue sections (4 μm) from paraffin blocks were stained immunohistochemically using a BOND-MAX Automated IHC/ISH Stainer (Leica Microsystems GmbH). All tissue blocks were fixed in 10% formalin at room temperature and embedded in paraffin for 24 h. Sections were mounted onto slides, air dried for 20 min and heated at 60˚C for 20 min. Sections were dewaxed twice with dewaxed solution (Celnovte Biotechnology Co., Ltd.) at 72˚C for 2 min, hydrated three times with anhydrous ethanol at room temperature for 2 min, and washed four times with washing solution (Celnovte Biotechnology Co., Ltd.) at room temperature for 6 min, The heat (98˚C)-induced antigen retrieval method was performed using Tris-EDTA buffer (1X; cat. no. K0071; Shanghai Jiehao Biotechnology Co., Ltd.) and endogenous peroxidase activity was quenched with 3% peroxidase-blocking reagent (Celnovte Biotechnology Co., Ltd.) at 37˚C for 5 min. The slides were incubated with the following commercially available antibodies at 37˚C for 30 min: Estrogen receptor (ER) (cat. no. CEM-0081; 1:500), progesterone receptor (PR) (cat. no. CPM-0365; 1:500), HER2 (cat. no. CCM-0844; 1:100); cytokeratin (CK)5/6 (cat. no. CCR-0982; 1:500), S100 (cat. no. CSM-0101; 1:500), GATA binding protein 3 (GATA3; cat. no. CGM-0130; 1:500), CK7 (cat. no. CCM-0992; 1:500), p63 (cat. no. CPM-0160; 1:100) and Ki-67 (cat. no. CKM-0032; 1:500; Table I). All antibodies were purchased from Celnovte Biotechnology Co., Ltd. Tissue sections were then washed twice with washing solution (Celnovte Biotechnology Co., Ltd.) for 6 min and incubated with Microstacker™ + Linker (cat. no. SD5300; 1:20; Celnovte Biotechnology Co., Ltd) at room temperature for 15 min for signal amplification. After washing twice with TBS for 6 min, samples were incubated with Microstacker™ Flex HRP-polymer detection reagent (cat. no. SD5100; 1:20; Celnovte Biotechnology Co., Ltd) at 37˚C for 30 min. After incubation with the polymer reagent, tissue sections were thoroughly washed three times with TBS buffer for 6 min and incubated with Microstacker™ DAB + Chromogen (cat. no. SD5300; 1:20; Celnovte Biotechnology Co., Ltd) at 37˚C for 6 min. Slides were washed twice with TBS buffer for 6 min, then counterstained with hematoxylin at 37˚C for 2 min and washed with TBS and dH_2O for 6 min, respectively. Dehydration using graded ethanol solutions and 90% xylene was performed, then sections were mounted in synthetic resin and observed under a BX53 light microscope (Olympus Corporation).

IHC results were scored by two independent observers according to the percentage of positively stained cells: i) 0+, 1-25% staining; ii) 1+, 26-50% staining; iii) 2+, 51-75% staining; and iv) 3+, 76-100% staining.

Fluorescence in situ hybridization (FISH). HER2 FISH was performed using the Kanglu HER2 DNA Probe Kit (Wuhan HealthCare Biotechnology Co., Ltd.) according to the manufacturer's protocols. Tissue blocks were fixed in 10% formalin at room temperature and embedded in paraffin for 24 h. For each tissue specimen, 4-μm sections were cut, deparaffinized, rehydrated in ethanol gradient and heated in a pretreatment solution of 2-(N-morpholino) ethanesulphonic acid at 95˚C for 10 min before being soaked twice in Tris/HCl buffer at room temperature for 3 min. The specimens were then digested in 200 μl pepsin (4 mg/ml; Guangzhou Anbiping Medical Technology Co., Ltd.) working solution at 37˚C for 45 min and agitated twice in Tris/HCl buffer at room temperature for 3 min. Slides were then dehydrated in an ascending ethanol series at room temperature and air-dried. Probe (10 μl; 500 ng/μl) was applied to each slide at 85˚C for 5 min and the hybridization area was covered with a coverslip. Co-denaturation of the probe and specimen was then performed at 85˚C for 5 min, before the slides were incubated at 37˚C for 10 h. The slides were washed in 2X saline-sodium citrate/0.1% NP-40 at 37˚C for 10 min and 10 μl DAPI counterstain was applied at 85˚C for 5 min before sealing. Slides were imaged using a Zeiss Imager Z2 fluorescence microscope using FISH imaging systems (V 1.3; GuangZhou MM Photoelectric Techology Co., Ltd.) software (Fluorescence microscope MF43-M (medical device model) + micro camera MC50-S/MS23+ fluorescent light source MG-100/MG-120/MG-200). The fluorescent signal in 20 cells from each slide was analyzed by two independent observers. FISH results were recorded as either negative or positive according to the American Society of Clinical Oncology/College of American Pathologists guideline by the two experienced pathologists independently in 20 tumor cells in a blinded manner (16).

For ETS variant transcription factor 6 *(ETV6)* FISH, 4-μm 10% formalin-fixed at room temperature for 24 h, paraffin-embedded tumor sections were heated at 60˚C for 1 h, rinsed in 100% ethanol and pretreated with 0.2 N HCl for 20 min at room temperature. Slides pretreatment, hybridization, washing and counterdyeing steps followed: Place slides in a 65±5˚C incubator for 24 h, room temperature in xylene

Table I. Primary antibodies and dilutions used for the immunohistochemical analyses and observed results.

				Results	
Antibody	Clone	Working dilution	Pretreatment	Case 1	Case 2
ER	C6H7	RTU	EDTA (pH=9.0)	Negative	Negative
PR	C4D10	RTU	EDTA (pH=9.0)	Negative	Negative
HER2	C1F7	RTU	EDTA (pH=9.0)	2+	2+
CK5/6	C6H1/C1C8	RTU	EDTA (pH=9.0)	Positive	Positive
S100	4C4.9	RTU	EDTA (pH=9.0)	Positive	Positive
GATA3	L50-823	RTU	EDTA (pH=9.0)	Positive	Negative
P63	C2C10	RTU	EDTA (pH=9.0)	Negative	Negative
Ki-67	C3G4	RTU	EDTA (pH=9.0)	30%+	55%+

CK, cytokeratin; ER, estrogen receptor; GATA3, GATA binding protein 3; PR, progesterone receptor; RTU, ready to use.

twice, 10 min each time → 100% ethanol at room temperature for 10 min → 90% ethanol at room temperature for 3 min → 70% ethanol at room temperature for 3 min → purified water at room temperature for 3 min → purified water at 100˚C for 25 min → pepsin (4 mg/ml; Guangzhou Anbiping Medical Technology Co., Ltd.) working solution at 37˚C for 15 min → 2xSSC at room temperature for 3 min → 70% ethanol at room temperature for 2 min → 90% ethanol at room temperature for 2 min → 100% ethanol at room temperature for 2 min → add probe (500 ng/μl; Guangzhou Anbiping Medical Technology Co., Ltd.) to the slides→ denature at 85˚C for 5 min → hybridization at 37˚C for 18 h → 0.1% NP-40/2X SSC at 37˚C for 5 min → 70% ethanol for at room temperature 3 min → hybrid blue staining solution at room temperature. Slides were imaged using a Zeiss fluorescence microscope (Carl Zeiss AG). IMSTAR software (version 2.0; ProgRes CT3, Jena, Germany) was used to analysis the results.

NGS. The two patients underwent molecular analysis using the Illumina NGS platform (Illumina, Inc.), which can detect mutations, copy number variations and fusions in 685 genes that are known to be oncogenic drivers (17). NGS was performed for the two patients using DNA from both tumor samples. NGS was performed according to Illumina's standard protocol. DNA was extracted using the MeiJi Tissue & Blood DNA Kit (cat. no. IVD3101-200; Guangzhou Magen Biotechnology Co., Ltd.) according to the manufacturer's protocol. A paired-end DNA library was prepared according to the manufacturer's protocol (Agilent Technologies, Inc.). Samples with >1 μg DNA were used for library preparation. Qubit quantification was used to verify the quality and integrity of samples and that the extraction amount was ≥50 ng. The loading concentration of the final library was 0.7 nM. The concentration of Cng/ul was measured by Qubit, and the average size of the library was double base pair) analyzed using the Agilent 4200 bioanalyzer (Agilent Technologies, Inc.). The molar concentration was calculated according to the formula: M=(Cng/μl x10^6)/(660 g/mol x D) nmol/l. Genomic DNA was fragmented using a sonicator (Covaris, LLC) to a length of 200-300 bp. The ends of the DNA fragments were then repaired, before the Illumina Adaptor was added (Fast Library Prep Kit; iGeneTech Bioscience Co., Ltd.) Using the 2003200-P2 Unique Dual Index Adapters (2 nmol) and KAPA Library Construction kit kk8514 (F. Hoffmann-La Roche Ltd; cat. no. 07962428001) KAPA Hyperplus Kit. The DNA fragments were end-polished, A-tailed and ligated with the full-length adapter. After the sequencing library was constructed, whole exomes were captured with the NadPrep Hybrid Capture Reagents (Nanodigmbio Biotechnology Co., Ltd.) and double-ended double-label sequenced using a Nextseq 6000 sequencer (Illumina, Inc.) with the NovaSeq 6000 S1 Reagent Kit v1.5 (300 cycles; cat. no. 20028317; Illumina, Inc.). The maximum sequencing read length was 2x150 bp (Paired-End 150 bp) and double-ended double-label sequencing was performed. Fastp software (version 0.11.9) (18) was used for quality control and preprocessing and the Burrows-Wheeler Aligner software (version 0.7.16) (19) was used to align clean reads with the hg19 reference genome. Mutect software (version 1.1.6) (20) was used to detect somatic variants in the tumor samples. Single nucleotide variants were annotated and filtered using snpEff software (version 5.1) (21).

Results

Clinical findings. The clinical data of the 2 patients were recorded (Table II). Both of the patients were female, and the patients were aged 42 and 69 years old at the time of diagnosis. Both patients reported the presence of a mass with no other complications. The preoperative duration was 3 days and 1 month for case 1 and case 2, respectively. Follow-up information was available for case 1 and case 2 for 16 and 14 months, respectively. After surgery, case 1 was administered with adjuvant chemotherapy of the TC taxel + Cyclophosphamide) scheme (120 mg/m^2 docetaxel and 800 mg/m^2 cyclophosphamide) intravenously every 3 weeks for 4 cycles. Subsequently, 1 year after surgery, the patient (case 1) developed a liver metastasis (Fig. S1), accompanied by lumbar vertebra and sacral vertebra metastasis. In addition, 15 months after surgery, the patient presented with ascites. Case 2 declined any further therapy and showed no recurrence or metastasis after surgery. Patients denied the use of novel antibody-drug conjugates (ADCs).

Table II. Clinical and histopathologic characteristics of patients with breast ACC.

Clinical characteristic	Case 1	Case 2
Patient sex	Female	Female
Age, years	42	69
Imaging size		
Lymph node status	0/9	0/23
Follow-up duration, months	16	14
Surgical treatment	Mastectomy and ALND	Mastectomy and ALND
Preoperative duration	3 days	1 month
Chemotherapy		
Neoadjuvant	No	No
Adjuvant	Yes	No
Adjuvant radiation	No	No
Growth pattern	Solid-trabecular	Solid-trabecular
DCIS	No	No
Recurrence	No	No
Site of distant metastasis	Liver, lumbar vertebra and sacral vertebra	Negative
Patient outcome	Alive	Alive
Tumor size, mm	50	25
Diagnosis	Pure ACC	Pure ACC

ACC, acinic cell carcinoma; ALND, axillary lymph node dissection; DCIS, ductal carcinoma *in situ*.

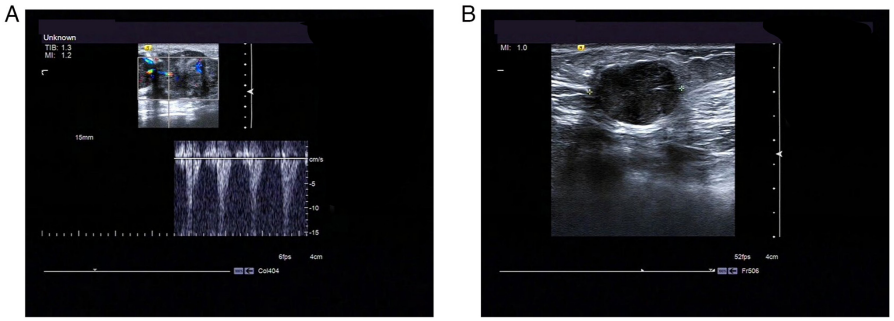

Figure 1. Characteristics of the breast acinic cell carcinoma observed on ultrasound scans. (A) Blood flow signal in the mass showed high resistance waveform in case 1. (B) The tumor tissue exhibited an irregular shape with clear boundaries and a strong dotted echo and blood flow signal could be observed in the mass in case 2. TIB, thermal index bone; MI, mechanical index; fps, frames per second; Col404, color 404.

Imaging findings. In case 1, a hypoechoic nodule of irregular shape with dimensions of ~4.6x2.3x2.7 cm was found in the left breast (‘6 o'clock’) beneath the nipple with unclear boundaries (Fig. 1A). The lesion was characterized as Breast Imaging Reporting and Data System (BI-RADS) category 4 (22).

In case 2, a hypoechoic mass measuring ~1.9x1.4x1.9 cm could be observed in the right breast (‘11 o'clock’), 2 cm away from the nipple. The tumor boundary was visible, and the shape was regular and was accompanied by a lateral sound shadow with a strong echo. Blood flow signals could be detected in the mass. The lesion was characterized as BI-RADS category 4 (Fig. 1B).

Pathological features

Macroscopic features. On gross examination, the tumor in case 1 was 55x40x30 mm in size, with a gray-white and rubbery consistency, had an ill-defined border and was moderately firm-hard to the touch (Fig. 2A). In case 2, there was a 30x25x20-mm tumor with a well-defined border that was moderately firm-hard and white-grey on the cut surface (Fig. 2B). There were no skin ulcerations, nipple changes or separate skin nodules in cases 1 and 2.

Microscopic features and IHC findings. Both of the tumors exhibited solid or nested growth patterns. The solid or nested growth patterns interconnected to form the burrowing labyrinthine network, ‘hand-holding-hand’ pattern or crawling phenomenon, which is similar to the carcinoma cuniculatum in the mandible (22) or the crawling carcinoma in the stomach (23) (Figs. 3A-E and 4A-E). The neoplastic cells exhibited abundant basophilic cytoplasm with centrally-located nuclei and prominent nucleoli, but also occasionally exhibited a clear cytoplasm (Figs. 3F and 4F).

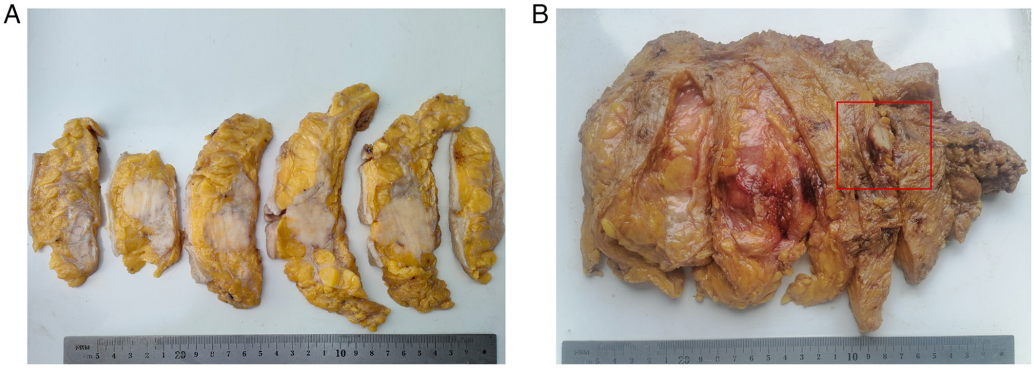

Figure 2. Macroscopic features of the tumor. (A) Tumor boundary was not well defined with a gray-white cut surface in case 1. (B) Following sectioning, the tumor was gray-white with a rubbery consistency and clear boundary (red box) in case 2.

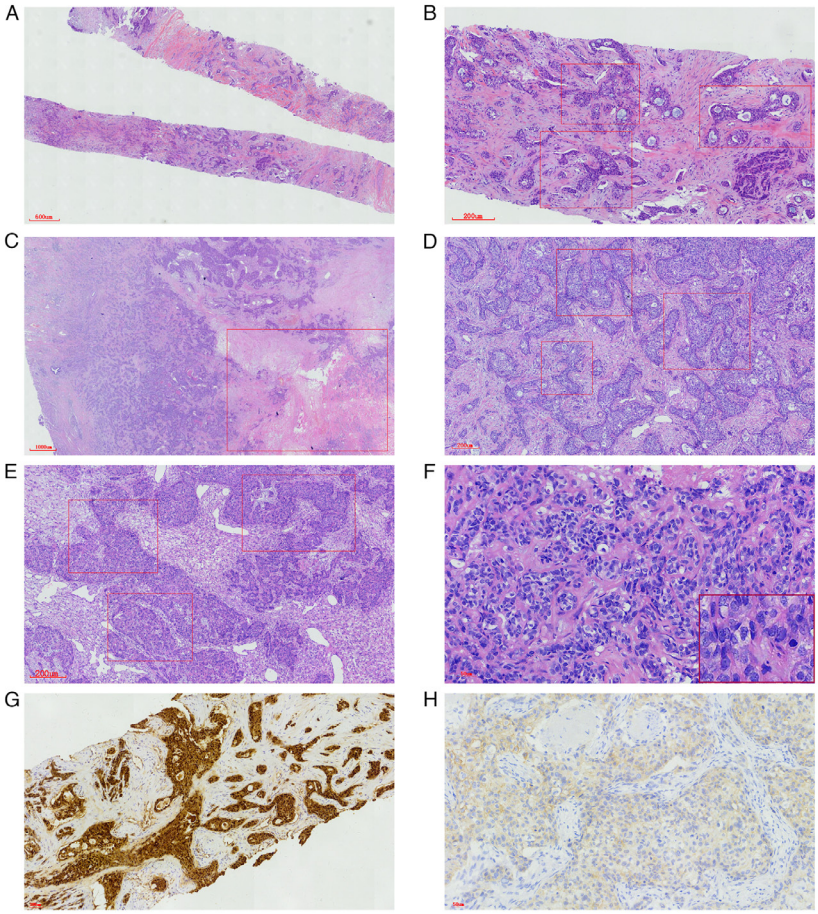

Figure 3. Staining results of the tumor tissue from case 1. Imaging of the tumor tissue demonstrated (A) invasive carcinoma (magnification, x18), (B) the 'hand-holding-hand' pattern of tumor cells (red box; magnification, x66), (C) the fibrotic focus (red box; magnification, x10), (D) the 'hand-holding-hand' pattern (red box; magnification, x50), (E) the 'hand-holding-hand' pattern (red box; magnification, x50) in another area, (F) cell characteristics of obvious atypia and mitotic figures (insert; magnification, x240), (G) positive S100 staining highlighting the 'hand-holding-hand' pattern (magnification, x78) and (H) human epidermal growth factor receptor-2 immunohistochemistry staining scored as 2+ (magnification, x150).

Atypia of tumor cells was prominent with marked mitotic figures (Figs. 3F and 4F insert). The cancer cells had high-grade nuclei with moderate-to-severe pleomorphism, coarse chromatin and a prominent singular nucleolus (Figs. 3F and 4F). An *in situ* component was not present either within or around the tumor. There were no invasive lymphocytes in the tumor tissues (Figs. 3A and 4A). Tumors were positive for S100 protein (Figs. 3G and 4G) in both patients. The neoplastic cells exhibited moderately positive (2+) HER2 expression (Fig. 3H and 4H). Both of the cases were CK5/6- (Fig. S2A and B) and CK7-positive (Fig. S2C and D). The tumor was positive for GATA3 in case 1 (Fig. S2E), but negative in case 2 (Fig. S2F). Staining for p63 (Fig. S2G and H), ER (Fig. S3A and B) and PR (Fig. S3C and D) was negative in both tumors. The Ki-67 index was 30% (Fig. S3E) and 55% (Fig. S3F) in the tumors from case 1 and case 2, respectively.

Table III. Gene mutations detected in case 1.

Gene	Exon	Nucleic acid variation	Amino acid change	Abundance, %
TP53BP1	11	NM_001141980.1; c.1362_1367del	p.I455_P456del	30.84
PALB2	8	NM_024675.3; c.2799del	p.C933Wfs*2	29.65
FGF3	3	NM_005247. 2; c.542G>A	p.R181H	24.15
ATRX	23	NM_000489.4; c.5690A>G	p.E1897G	22.16
MTOR	46	NM_004958.3; c.6414G>T	p.L2138F	11.62
KLHL6	7	NM_130446.2; c.1589C>G	p.A530G	5.78
CCNE1	7	NM_001238.3; c.479A>G	p.K160R	3.09
MED12	27	NM_005120.2; c.3817G>T	p.A1273S	2.17
ELF3	5	NM_004433.4; c.485G>A	p.G162D	1.08

Table IV. Gene mutations detected in case 2.

Gene	Exon or intron	Nucleic acid variation	Amino acid change	Abundance, %
TP53	Exon 4	NM_000546.5; c.323del	p.G108Vfs*15	78.19
NSD1	Exon 5	NM_022455.4; c.3157A>T	p.K1053*	34.37
SPEN	Exon 11	NM_015001.2; c.7480C>T	p.P2494S	31.45
DOT1L	Exon 25	NM_032482.2; c.3580G>A	p.E1194K	30.84
RET	Exon 3	NM_020975.4; c.538C>T	p.R180*	19.38
JAK3	Exon 23	NM_000215.3; c.3118T>A	p.C1040S	18.84
MAP3K14	Exon 2	NM_003954.4; c.115G>A	p.V39I	9.40
MED12	Exon 27	NM_005120.2; c.3817G>T	p.A1273S	3.25
KMT2C	Intron 13	NM_170606.2; c.1814-1G>A	p.?	3.17

Molecular analysis demonstrated mutations in mediator of RNA polymerase II transcription, subunit 12 homolog (MED12) exon 27. Targeted NGS results from case 1 demonstrated the presence of mutations in the tumor protein p53 binding protein 1 (NM_001141980.1; c.1362_1367del; p.I455_P456del), partner and localizer of breast cancer 2 (NM_024675. 3; c.2799del; p.C933Wfs*2), fibroblast growth factor 3 (NM_005247.2; c.542G>A; p.R181H), α thalassemia/mental retardation syndrome X-linked (NM_000489.4; c.5690A>G; p.E1897G), *mTOR* (NM_004958.3; c.6414G>T; p.L2138F), Kelch-like protein 6 (NM_130446.2; c.1589C>G; p.A530G), cyclin E1 (NM_001238.3; c.479A>G; p.K160R), *MED12* (NM_005120.2; c.3817G>T; p.A1273S; abundance, 2.17%) and E74-like ETS transcription factor 3 (NM_004433.4; c.485G>A; p.G162D) genes.

The gene mutations present in case 2 included *TP53* (NM_000546.5; c.323del; p.G108Vfs*15), nuclear receptor-binding SET domain 1 (NM_022455.4; c.3157A>T; p.K1053*), spen family transcription repressor (NM_015001.2; c.7480C>T; p.P2494S), disruptor of telomeric silencing 1-like (NM_032482.2; c.3580G>A; p.E1194K), rearranged in transfection (NM_020975.4; c.538C>T; p.R180*), janus kinase 3 (NM_000215.3; c.3118T>A; p.C1040S), mitogen-activated protein kinase kinase kinase 14 (NM_003954.4; c.115G>A; p.V39I), *MED12* (NM_005120.2; c.3817G>T; p.A1273S; abundance, 3.25%) and lysine methyltransferase 2C (NM_170606.2; c.1814-1G>A; p.*). The *MED12* exon 27 mutation was found in both cases (Tables III and IV).

FISH results. FISH showed the average copy number of the red signal/average copy number of the green signal in case one and case two was 1.0 and 1.11, respectively, and revealed that the tumor tissues in the two case were negative for HER2 amplification (Fig. S4A and B). The two cases showed 2G(green signal)2R(red signal) signal mode and indicated no *ETV6* break-apart probe detection (Fig. S4C and D).

Discussion

Invasive breast carcinoma is an umbrella term used for a large and heterogeneous group of malignant epithelial neoplasms of the glandular elements in the breast (10). Breast ACC is a rare type of invasive breast cancer that typically has a benign course (8,9). However, occasionally breast ACC can progress into high-grade TNBC (9,10). To the best of our knowledge, the present study was the first to focus on the relationship between the structure of breast ACC and gene alterations. In addition, the microstructure of the breast ACC in CNB samples was probed, supplementing the cellular features assessed, such that structures in the CNB and surgically excised samples were compared. Beca *et al* (12) previously reported that breast ACCs were genetically heterogeneous and displayed genomic features overlapping those of the common forms of

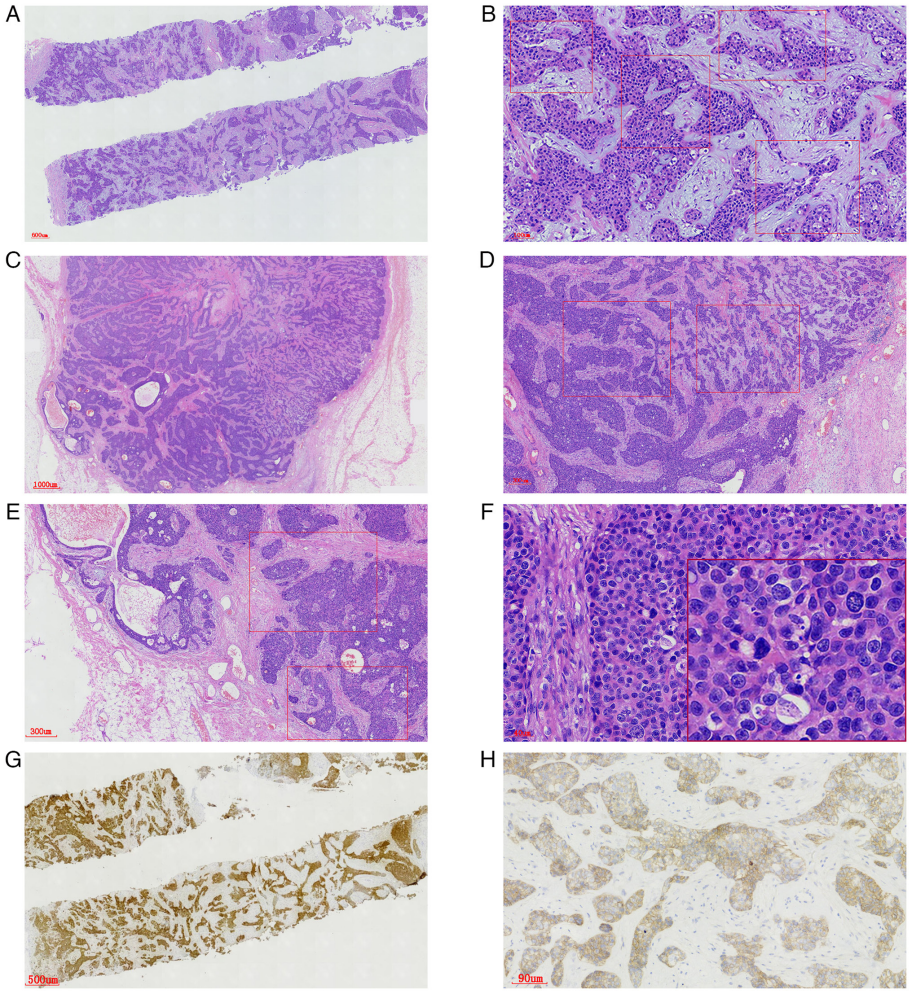

Figure 4. Staining results of the tumor tissue from case 2. Imaging of the tumor tissue demonstrated (A) invasive carcinoma (magnification, x20), (B) the 'hand-holding-hand' pattern of tumor cells (red box; magnification, x120), (C) the clear boundary of the tumor (magnification, x010), (D) the 'hand-holding-hand' pattern (red box; magnification, x35), (E) the 'hand-holding-hand' pattern (red box; magnification, x35) in another area, (F) cell characteristics of obvious atypia and mitotic figures (insert; magnification, x260), (G) positive S100 staining and the 'hand-holding-hand' pattern (magnification, x78) and (H) human epidermal growth factor receptor-2 immunohistochemistry staining scored as 2+ (magnification, x150).

TNBC (12). Furthermore, breast ACCs were not likely to be driven by a highly recurrent mutation or oncogenic gene fusion events (12).

In the present study, the CNB samples and lumpectomy specimens were compared. It was demonstrated that both cases showed the same histological and IHC features. Specifically, both sets of tissues exhibited a solid or nest interconnecting structures and formed a burrowing labyrinthine network, similar to the carcinoma cuniculatum of the oral cavity (23) or branching and anastomosing structure, similar to 'hand-shaking-hand' pattern or crawling phenomenon in well-differentiated gastric adenocarcinoma of intestinal type (24). There was no carcinoma *in situ* in the center or around the invasive components, and no tubular or microglandular structures were found. However, it was demonstrated that the cancer cells did have high-grade nuclei of moderate-to-severe pleomorphism, coarse chromatin and a prominent singular nucleolus. These tumor cells also had uniform basophilic cytoplasm and the finely to coarsely granular chromatin were not obvious. There were no or few mononucleated lymphoid cells infiltrating into the tumor cells and stroma, although there was marked hyalinization in the stromal component. The tumors were negative for ER, PR and p63, and positive for S100, CK5/6 and CK7. The tumor cells stained moderately positive (2+) for HER2, but no HER2 amplification could be detected by FISH. Therefore, burrowing labyrinthine networks, hand-holding-hand pattern or crawling phenomenon as structures and basophilic cytoplasm as a cytological feature are likely to be unique to ACC CNB or surgically excised samples. Although ACC can be misdiagnosed as a secretory carcinoma, it typically presents with a bland nuclear morphology and harbors ETV6-neurotrophic receptor tyrosine kinase 3 fusions, which were absent in the present study.

According to the genomic analyses of the 2 patients in the present study, the tumors demonstrated *MED12* exon 27 mutations. *MED12* is an X chromosome-linked gene that encodes the protein mediator complex subunit 12 (25). Mediator complex subunit 12 is a large multi-subunit complex that is critical for gene regulation (24). *MED12* mutations have been identified in 80% of phyllodes tumors with little variance in frequency among malignant, benign and borderline tumors (26). In addition, *MED12* mutations have been previously reported in breast cancer (27). Conlon *et al* (28) previously reported missense mutations in the *MED12* gene (*D1204E*) with lower

allelic frequencies in 1 case of breast ACC (27). However, both of the cases in the present study displayed mutations in exon 27 (NM_005120.2; c.3817G>T; p.A1273S). In addition, *MED12* mutations detected in these patients exhibited a similar abundance. Therefore, *MED12* exon 27 mutations may be associated with the burrowing labyrinthine network or 'hand-holding-hand' structure of breast ACC.

According to IHC results, all invasive breast cancers are grouped into the following biomarker-defined subtypes/groups for treatment purposes on the basis of the HER2 status: i) ER-positive, HER2-negative; ii) ER-positive, HER2-positive; iii) ER-negative, HER2-positive; or iv) ER-negative, HER2-negative (10). HER2-negative tumors are further categorized into HER2-0 (IHC staining score of 0) and HER2-low (IHC staining score of 1+ or 2+ combined with FISH-negative results) (29). ADCs have been used effectively in patients with low HER2 protein expression (30). The patients in the present study were grouped into the HER2-low breast cancer category, although the tumors were HER2-negative according to the FISH results. However, the patients refused the use of ADCs.

The prognosis of patients with breast ACC remains uncertain. A previous case report suggested that breast ACC is likely to have a good prognosis (15). However, it is clear that poorly differentiated TNBC can become a component of breast ACC and recurrence and mortality can occur (14). It could be suggested that prognosis is predominantly driven by the presence of the poorly differentiated component. The 2 cases in the present study exhibited high-grade cell features. However, the patient from case 1 had a poor prognosis and the patient from case 2 appeared to have a superior outcome. Although case 1 was administered adjuvant chemotherapy of the TC scheme 10 days after surgery, and 1 year after surgery, the patient developed a liver, lumbar vertebra and sacral vertebra metastasis and 15 months later presented with ascites after surgery. And Case two declined any further therapy and showed no recurrence or metastasis after surgery. This diverse prognostic observation may be related to the fibrotic focus (31).

The present study had several limitations. The present study was retrospectively designed, which could cause certain selection bias. In addition, only 2 breast ACC cases were described in the present study.

In summary, the present study demonstrated a rare structure of breast ACC with a burrowing labyrinthine network or 'hand-holding-hand' feature. The key to accurate diagnosis is the combination of knowledge of tumor type, recognition of the characteristic morphology and IHC profile. The same gene mutation with a similar abundance in *MED12* exon 27 (NM_005120.2; c.3817G>T; p.A1273S) was reported in both tumors. Therefore, the *MED12* exon 27 mutation may potentially be associated with the formation of a burrowing labyrinthine network or the 'hand-holding-hand' feature observed in the present study. Future studies with larger sample sizes are required to further investigate this potential genotype-phenotype association in breast ACC.

Acknowledgements

Not applicable.

Funding

The present study was supported by a grant from the People's Liberation Army 989 Hospital Foundation (grant no. 9892023YNKT-04A).

Availability of data and materials

The NGS datasets generated and/or analyzed during the current study are available in the NCBI Sequence Read Archive repository, https://www.ncbi.nlm.nih.gov/sra/PRJNA1025041. The other datasets used and/or analyzed during the current study are available from the corresponding author on reasonable request.

Authors' contributions

CL, GL, XX, ZL, FL and XY designed the study. ZL, XX, MZ, YaL, XY and XG recruited the patients. CL, GL, FL, ZL, ZC, CZ, XY, MZ, YaL, PW, YuL and XG analyzed the experimental data and composed all figures and tables. CL, FL, ZL and HY wrote the manuscript. ZC, XG, MZ and FL confirm the authenticity of all the raw data. All authors read and approved the final version of the manuscript.

Ethics approval and consent to participate

The present study was approved by the 989 Hospital Medical Ethics Committee (Luoyang, China; ethics approval no. WZLL-2023-016) and Fenlan Lab Medical Ethics Committee (Hangzhou, China; ethics approval no. 2023-06). Written informed consent was obtained from the patients at the time of the initial data collection for participation in the study.

Patient consent for publication

The patients provided written informed consent for publication of patient data and associated images.

Competing interests

The authors declare that they have no competing interests.

References

1. Sung H, Ferlay J, Siegel RL, Laversanne M, Soerjomataram I, Jemal A and Bray F: Global cancer statistics 2020: GLOBOCAN estimates of incidence and mortality worldwide for 36 cancers in 185 countries. CA Cancer J Clin 71: 209-249, 2021.
2. Ordóñez NG: Pancreatic acinar cell carcinoma. Adv Anat Pathol 8: 144-159, 2001.
3. Holen KD, Klimstra DS, Hummer A, Gonen M, Conlon K, Brennan M and Saltz LB: Clinical characteristics and outcomes from an institutional series of acinar cell carcinoma of the pancreas and related tumors. J Clin Oncol 5: 4673-4678, 2002.
4. Rodriguez J, Diment J, Lombardi L, Dominoni F, Tench W and Rosai J: Combined typical carcinoid and acinic cell tumor of the lung: A heretofore unreported occurrence. Hum Pathol 34: 1061-1065, 2003.
5. Hervieu V, Lombard-Bohas C, Dumortier J, Boillot O and Scoazec JY: Primary acinar cell carcinoma of the liver. Virchows Arch 452: 337-341, 2008.
6. Ambrosini-Spaltro A, Potì O, De Palma M and Filotico M: Pancreatic-type acinar cell carcinoma of the stomach beneath a focus of pancreatic metaplasia of the gastric mucosa. Hum Pathol 40: 746-749, 2009.

7. Pesci A, Castelli P, Facci E, Romano L and Zamboni G: Primary retroperitoneal acinar cell cystadenoma. Hum Pathol 43: 446-450, 2012.
8. Roncaroli F, Lamovec J, Zidar A and Eusebi V: Acinic cell-like carcinoma of the breast. Virchows Arch 429: 69-74, 1996.
9. Guerini-Rocco E, Hodi Z, Piscuoglio S, Ng CK, Rakha EA, Schultheis AM, Marchiò C, da Cruz Paula A, De Filippo MR, Martelotto LG, *et al*: The repertoire of somatic genetic alterations of acinic cell carcinomas of the breast: An exploratory, hypothesis-generating study. J Pathol 237: 166-178, 2015.
10. WHO Classification of Tumors Editorial Board. Breast tumours. WHO Classification of Tumors. 5th edition. Lyon, IARC, 2019.
11. Geyer FC, Berman SH, Marchio C, Burke KA, Guerini-Rocco E, Piscuoglio S, Ng CK, Pareja F, Wen HY, Hodi Z, *et al*: Genetic analysis of microglandular adenosis and acinic cell carcinomas of the breast provides evidence for the existence of a low-grade triple-negative breast neoplasia family. Mod Pathol 30: 69-84, 2017.
12. Beca F, Lee SSK, Pareja F, Da Cruz Paula A, Selenica P, Ferrando L, Gularte-Mérida R, Wen HY, Zhang H, Guerini-Rocco E, *et al*: Whole-exome sequencing and RNA sequencing analyses of acinic cell carcinomas of the breast. Histopathology 75: 931-937, 2019.
13. Collins LC, Connolly JL, Page DL, Goulart RA, Pisano ED, Fajardo LL, Berg WA, Caudry DJ, McNeil BJ and Schnitt SJ: Diagnostic agreement in the evaluation of image-guided breast core needle biopsies: Results from a randomized clinical trial. Am J Surg Pathol 28: 126-31, 2004.
14. Ajkunic A, Skenderi F, Shaker N, Akhtar S, Lamovec J, Gatalica Z and Vranic S: Acinic cell carcinoma of the breast: A comprehensive review. Breast 66: 208-216, 2022.
15. Cima L, Kaya H, Marchiò C, Nishimura R, Wen HY, Fabbri VP and Foschini MP: Triple-negative breast carcinomas of low malignant potential: Review on diagnostic criteria and differential diagnoses. Virchows Arch 480: 109-126, 2022.
16. Wolff AC, Hammond MEH, Allison KH, Harvey BE, Mangu PB, Bartlett JMS, Bilous M, Ellis IO, Fitzgibbons P, Hanna W, *et al*: Human epidermal growth factor receptor 2 testing in breast cancer: American Society of Clinical Oncology/College of American pathologists clinical practice guideline focused update. J Clin Oncol 36: 2105-2122, 2018.
17. Abdel-Salam EM, Faisal M, Alatar AA, Qahtan AA and Alam P: Genome-wide transcriptome variation landscape in Ruta chalepensis organs revealed potential genes responsible for rutin biosynthesis. J Biotechnol. Jan 325: 43-56, 2021.
18. Chen S, Zhou Y, Chen Y Gu J: fastp: An ultra-fast all-in-one FASTQ preprocessor. Bioinformatics 34: i884-i890, 2018.
19. Li H and Durbin R: Fast and accurate short read alignment with Burrows-Wheeler transform. Bioinformatics 25: 1754-1760, 2009.
20. Cibulskis K, Lawrence MS, Carter SL, Sivachenko A, Jaffe D, Sougnez C, Gabriel S, Meyerson M, Lander ES and Getz G: Sensitive detection of somatic point mutations in impure and heterogeneous cancer samples. Nat Biotechnol 31: 213-219, 2013.
21. Yen JL, Garcia S, Montana A, Harris J, Chervitz S, Morra M, West J, Chen R and Church DM: A variant by any name: Quantifying annotation discordance across tools and clinical databases. Genome Med 9: 7, 2017.
22. Magny SJ, Shikhman R and Keppke AL: Breast Imaging Reporting and Data System. 2022 Aug 29. In: StatPearls. StatPearls Publishing, Treasure Island, FL, 2023.
23. Thavaraj S, Cobb A, Kalavrezos N, Beale T, Walker DM and Jay A: Carcinoma cuniculatum arising in the tongue. Head Neck Pathol 6: 130-134, 2012.
24. Ushiku T, Arnason T, Ban S, Hishima T, Shimizu M, Fukayama M and Lauwers GY: Very well-differentiated gastric carcinoma of intestinal type: Analysis of diagnostic criteria. Mod Pathol 26: 1620-1631, 2013.
25. Gonzalez CG, Akula S and Burleson M: The role of mediator subunit 12 in tumorigenesis and cancer therapeutics. Oncol Lett 23: 74, 2022.
26. Yoshida M, Sekine S, Ogawa R, Yoshida H, Maeshima A, Kanai Y, Kinoshita T, Ochiai A: Frequent MED12 mutations in phyllodes tumours of the breast. Br J Cancer 112: 1703-1708, 2015.
27. Banerji S, Cibulskis K, Rangel-Escareno C, Brown KK, Carter SL, Frederick AM, Lawrence MS, Sivachenko AY, Sougnez C, Zou L, *et al*: Sequence analysis of mutations and translocations across breast cancer subtypes. Nature 486: 405-409, 2012.
28. Conlon N, Sadri N, Corben AD and Tan LK: Acinic cell carcinoma of breast: morphologic and immunohistochemical review of a rare breast cancer subtype. Hum Pathol 51: 16-24, 2016.
29. Tarantino P, Hamilton E, Tolaney SM, Cortes J, Morganti S, Ferraro E, Marra A, Viale G, Trapani D, Cardoso F, *et al*: HER2-Low breast cancer: Pathological and clinical landscape. J Clin Oncol 38: 1951-1962, 2020.
30. Banerji U, van Herpen C, Saura C, Thistlethwaite F, Lord S, Moreno V, Macpherson I, Boni V, Rolfo C, de Vries E, *et al*: Trastuzumab duocarmazine in locally advanced and metastatic solid tumours and HER2-expressing breast cancer: A phase 1 dose-escalation and dose-expansion study. Lancet Oncol 20: 1124-1135, 2019.
31. Jeong YJ, Park SH, Mun SH, Kwak SG, Lee SJ and Oh HK: Association between lysyl oxidase and fibrotic focus in relation with inflammation in breast cancer. Oncol Lett 15: 2431-2440, 2018.